PREPARAREA ELECTROLITULUI SOLID DE TIP (La,Sr)(Ga,Mg)O_3 PRINTR-O METODĂ ÎMBUNĂTĂȚITĂ A REACȚIILOR ÎN FAZĂ SOLIDĂ
PROCESSING OF (La,Sr)(Ga,Mg)O_3 SOLID ELECTROLYTE USING AN ENHANCED SOLID STATE TECHNIQUE

VICTOR FRUTH*, CRISTIAN ANDRONESCU, CRISTIAN HORNOIU, ECATERINA ȚENEA, ADRIANA RUSU, RAREŞ SCURTU

Institutul de Chimie - Fizică "Ilie Murgulescu" al Academiei Române, Splaiul Independeței nr. 202, 060021, Bucureşti, România

Sr and Mg doped lanthanum gallate perovskites ($La_{1-x}Sr_xGa_{1-y}Mg_yO_{3-\delta}$) shortened as LSGM are promising electrolyte materials for intermediate temperature solid oxide fuel cells (IT-SOFCs).

The evolution of secondary phases, such as $LaSrGa_3O_7$ has been identified to be a problem in the preparation of LSGM. Actually, no mater what technical preparation route was adopted (wet-based or solid state-based method) the presence of the secondary phases, accompanying the main phase LSMG was reported.

The results regarding an attempt to obtain pure Sr and Mg doped $LaGaO_3$ ceramics using a specific annealing treatment was reported in this work. The obtained ceramics were characterized using different techniques. Thermal analyses (DTA/TG) on the stoichiometric raw mixture and dilatometric measurements on sintered bodies were performed. Morphological and structural aspects were investigated by means of X-ray diffractometry, FT-IR spectroscopy and scanning electron microscopy. The electrical behavior of the obtained ceramic was characterized by complex impedance spectroscopy.

Choosing an appropriate annealing program, almost pure Sr and Mg doped $LaGaO_3$ can be obtained.

Perovskiții de tip lantanat de galiu dopați cu Sr şi Mg ($La_{1-x}Sr_xGa_{1-y}Mg_yO_{3-\delta}$), abreviat LSGM, sunt electroliți promițători pentru pilele de combustie cu electrolit solid de temperaturi intermediare (IT-SOFC).

O problemă frecvent întâlnită la prepararea electroliților de tip LSGM constă în apariția unor faze secundare, precum faza $LaSrGa_3O_7$. În fapt, indiferent de metoda de preparare folosită (metoda pe bază de precursori lichizi sau metoda reacțiilor în stare solidă), literatura de specialitate raportează prezența fazelor secundare care însoțesc faza principală LSGM.

Această lucrare prezintă rezultatele încercării noastre de a obține, printr-o metodă îmbunătățită, materiale ceramice pure de $LaGaO_3$ dopate cu Sr şi Mg. Materialele ceramice obținute au fost caracterizate folosind mai multe tehnici. Astfel, amestecul stoichiometric inițial a fost investigată cu ajutorul analizei termice iar după sinterizare s-au realizat măsurători de dilatometrie. Caracteristicile structurale şi morfologice au fost investigate cu ajutorul difracției de raze X, spectroscopiei FT-IR şi microscopiei electronice cu baleaj. Proprietățile electrice ale corpurilor ceramice obținute au fost caracterizate prin spectroscopia de impedanță.

Folosind un program de tratament termic adecvat se pot obține materiale ceramice de tip $LaGaO_3$ dopate cu Sr şi Mg aproape pure.

Keywords: *solid electrolytes, Sr and Mg doped $LaGaO_3$, solid state technique, electric properties.*

1. Introduction

Perovskite-type ABO_3 phases derived from lanthanum gallate, $LaGaO_3$, possess a higher ionic conductivity than that of stabilized zirconia. Sr and Mg doped lanthanum gallate perovskites ($La_{1-x}Sr_xGa_{1-y}Mg_yO_{3-\delta}$, shortened as LSGM-XY where X and Y are the doping levels in mole percentage (mol%) at the La- or A-site and the Ga- or B-site, respectively) are promising electrolyte materials for intermediate temperature solid oxide fuel cells (IT-SOFCs) [1-11]. Compared with CeO_2-based electrolytes (which are also of interest for lowering the operating temperature of SOFCs), the electrolytic domain of doped $LaGaO_3$ extends to substantially lower oxygen chemical potentials [12-14]. For the LSGM series, the maximum ionic transport is achieved at x=0.10–0.20 and y=0.15–0.20 [15]; further acceptor-type doping leads to progressive vacancy association processes.

However, the concentration of transition metal dopants should be limited to below 3–7% as further additions lead to increasing electronic and decreasing ionic conductivities [16].

Disadvantages of $LaGaO_3$-based materials include possible reduction and volatilization of gallium oxide, formation of stable secondary phases during the processing, the relatively high cost of gallium and significant reactivity with perovskite electrodes under oxidizing conditions as well as with metal anodes in reducing conditions. These problems may be, to some extent, suppressed by the optimization of processing techniques.

The evolution of secondary phases, such as $LaSrGa_3O_7$ has been identified to be a problem in the preparation of LSGM. Actually, no mater what technical preparation route was adopted (wet-based or solid state-based method) the presence of the secondary phases, accompanying the main phase

* Autor corespondent/Corresponding author,
Tel: +40213188595/594, e-mail: vfruth@icf.ro

LSMG were signaled in literature [2,3,5,10,11].

In this work one obtain, by solid-state technique, a pure Sr and Mg doped $LaGaO_3$ ceramics using a specific annealing treatment.

2. Experimental and Characterization

Solid-state reaction (SSR) was chosen as synthesis route as it is the most commonly used technique in ceramic preparations. High pure compounds La_2O_3, $SrCO_3$, Ga_2O_3, $4MgCO_3.Mg(OH)_2{\times}5H_2O$ were used as starting components. Stoichiometric amounts ($La_{0.8}Sr_{0.2}Ga_{0.8}Mg_{0.2}O_{3-x}$) were mixed in agate mortar, following by the calcinations and sintering.

The green powder was first calcined at 1000ºC for 6 h. A heating rate of 5ºC/min was adopted up to 600ºC and then 1ºC/min up to 1000ºC was used. The calcined powders were pressed uni-axially into cylindrical shape samples (ϕ=10 mm, h=2-3 mm). The compacts were then sintered in air box furnace at 1450ºC and 1500ºC respectively, for 6h.

The densities of sintered samples at 1500ºC/6h (ρ~5.96 g/cm3) and porosity (~1.0 %) were measured using the standard Archimedes method.

The structure of the obtained materials was determined by X-ray diffraction (Rigaku ULTIMA IV Diffractometer, $Cu_{K\alpha}$). The search for impurity phases included the following substances: $LaSrGaO_4$ (Powder Diffraction File (PDF) No. 24–1208), $SrLaGa_3O_7$ (PDF No. 45-0637), $La_4Ga_2O_9$ (PDF No. 37–1433), $SrGa_2O_4$ (PDF No. 72-0222), $La_2O_{2.3}(CO_3)_{0.85}$ (PDF No. 84-1964).

IR (infrared) spectra were recorded using a Thermo NICOLET FTIR 6700 spectrometer. Thermal analysis (DTA/TG) was performed with a METTLER Toledo 851^e Derivatograph. Thermal expansion coefficients (TEC) were measured using a Netzsch DIL 402 C dilatometer, constant heating rate of 5ºC/min, in N_2. The morphology was determined by Scanning Electron Microscopy SEM (Zeiss DSM 942). The electrical behavior of the ceramic was characterized by impedance spectroscopy (Wayne Kerr 6440A) at frequencies in the range 20 Hz-3MHz with V_{ac}=1V. The measurements were carried out in air from room temperature up to 500°C. The pellets were coated with silver paste on both surfaces and then were heated at 300°C for 1 hour for a good contact with the electrode.

3. Results and discussion.

It is difficult to remove impurity phases (such as $LaSrGa_3O_7$) in the synthesis process of the Sr- and Mg-doped $LaGaO_3$, no matter what technique is employed. In fact, synthesis of a pure single phase of LSGM is rather hard to achieve [17]. Previous works concluded that, independently of preparation routes, calcination up to 1500ºC is necessary to obtain a pure perovskite phase [18], because $LaSrGa_3O_7$ and less $LaSrGaO_4$ are in thermodynamic equilibrium with LSGM at 1400ºC in air [19,20]. Another reason is the narrow composition range for the stability of the perovskite phase [21]. The solubility of Sr^{2+} on the La^{3+} sites in $LaGaO_3$ system is below 5 % for a sintering temperature of 1500ºC. The solubility limit of Sr^{2+} on the La^{3+} sites increases by substituting Mg^{2+} on the Ga^{3+} sites in $LaGaO_3$ [22]. The results of Ishihara et al. [9] showed also that incorporation of the guest ions in the host lattice at specific sites is realized by substitution mechanism. The bulk diffusion coefficients are similar for all cations with activation energies which are strongly dependent on temperature. It was found that diffusion takes place through the bulk and along the grain boundaries [23,24].

Taking into consideration the above observations one can conclude that reactions taking place in the subsolidus domain in the corresponding phase diagram of the doped La_2O_3-Ga_2O_3 system may play a significant role in preventing (hindering) the parasite phase formation. Starting with carbonates as raw materials may constitute an advantage. The alkaline earth carbonates, MCO_3 (M = Ca, Sr, and Ba), have several interesting properties. At certain temperatures, the MCO_3 would transform polymorphically the structure by the rotational disorder transition of the anion group at a certain temperature, such as the transformation of $CaCO_3$ from orthorhombic to hexagonal at 470ºC, $SrCO_3$ from orthorhombic to hexagonal at 950ºC, and $BaCO_3$ from orthorhombic to hexagonal at 800ºC (further to cubic at 970ºC) [25]. On the other hand, the thermal decomposition temperature of the carbonates can be lowered drastically by adding certain oxides. For instance, the thermal decomposition temperature of $SrCO_3$ was lowered from 1150ºC to 1102ºC by adding a specific amount of Al_2O_3 [26]. At temperature higher than the $SrCO_3$ transformation temperature, 950ºC, the solid-state reaction is dominated by diffusion of ions in the $SrCO_3$ lattice. Cations diffusion can be enhanced by the orthorhombic to hexagonal transformation of $SrCO_3$ because the high-temperature modification has a lower density. On the other hand a kinetic study of $SrCO_3$ decomposition in the solid-state reaction reveals that the activation energy of $SrCO_3$ decomposition was influenced by the calcination temperature rather than the nature of precursor. The interfacial reaction at low temperatures is characterized by a high activation energy of 130 kJ/mol, whereas, in the reactions at higher temperatures the activation energy of $SrCO_3$ decomposition decreases drastically to 34 kJ/mol.[27]. $MgCO_3$ decomposed at 450-550ºC and $SrCO_3$ above 1000ºC so the dopants are released gradually in the system.

Thermal decomposition of hydromagnesite 4 $MgCO_3.Mg(OH)_2x5H_2O$ proceeds via dehydration (< 300ºC) and decarbonation (>350ºC) towards MgO. The decarbonation is highly dependent on the partial pressure of carbon dioxide [28] (fig1.a).

From the figure 1.b it can be underlined that the decomposition of $SrCO_3$ started at arround

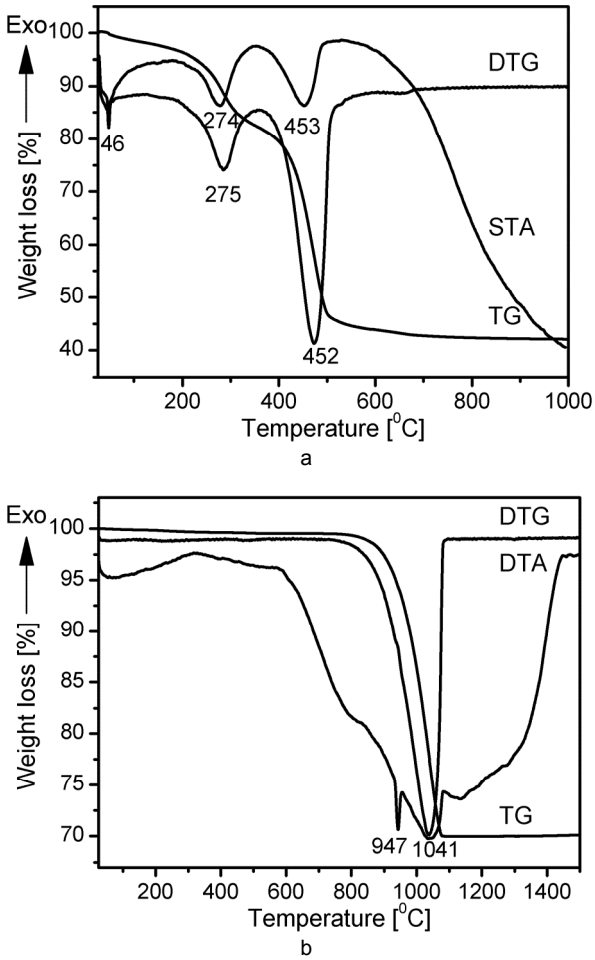

Fig. 1 - DTA and TG curves of $4MgCO_3.Mg(OH)_2×5H_2O$ (a) and $SrCO_3$ (b) raw materials / *Curbele ATD/TG ale $4MgCO_3.Mg(OH)_2×5H_2O$ (a) şi respectiv $SrCO_3$ (b).*

900ºC and is finished at 1100ºC. The endothermal event at 947ºC is attributable to the phase transition of Sr carbonate (orthorhombic to hexagonal)

By controlling the conversion rate of strontium carbonate (decomposition) one could try favoring the incorporation of Sr^{2+} for La^{3+} sites in LSGM phase.

Considering the differential thermal analysis DTA/TG (thermogravimetry) results of stoichiometric $La_{0.8}Sr_{0.2}Ga_{0.8}Mg_{0.2}O_{3-x}$ starting mixture with two heating rates, presented in figure 2, one can mention at least four weight loss distinct regions determined mainly by the elimination of adsorbed and crystalline water (up to 345ºC), and decomposition of carbonates at 450-550ºC for $MgCO_3$ and 750-940ºC for $SrCO_3$ respectively. The lower temperature for the last reaction is explained by the influence of other components of the system

(especially the presence of Mg^{2+} cations). Above 940ºC no weight loss can be observed. It is worth to mention some endothermal events recorded on DTA curve at 849ºC, 960ºC, 1260ºC, 1352ºC, 1425ºC and 1440ºC respectively, assigned to the reactions which occurred in nonisotermal conditions when the heating rate was 5ºC/min.

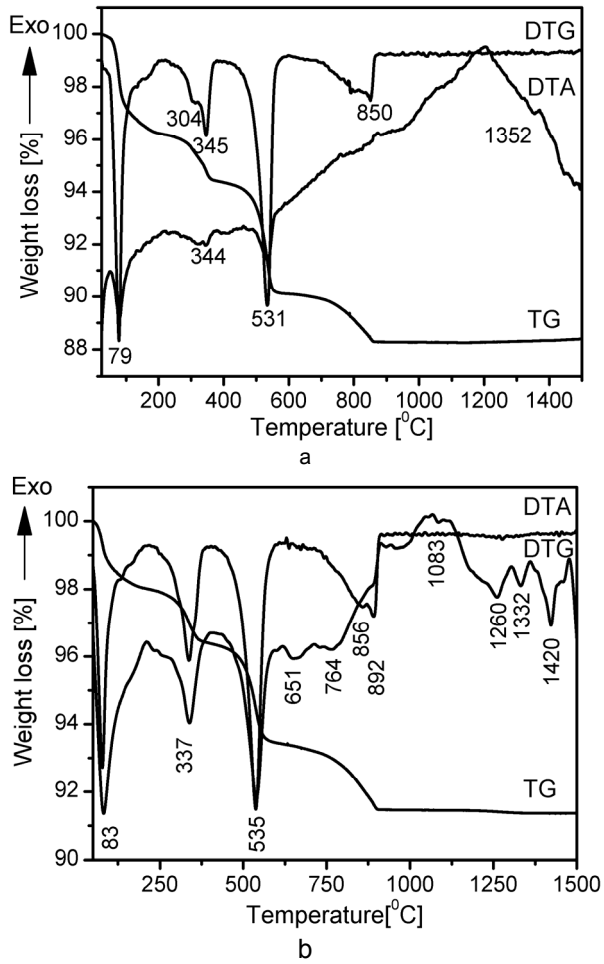

Fig 2 - DTA and TG curves of stoichiometric of $La_{0.8}Sr_{0.2}Ga_{0.8}Mg_{0.2}O_{3-x}$ starting mixture for two heating rate: 10ºC/min (a) and 5ºC/min (b) / *Curbele ATD/TG ale amestecului stoichiometric inițial $La_{0.8}Sr_{0.2}Ga_{0.8}Mg_{0.2}O_{3-x}$ pentru două viteze de încălzire: 10ºC/min (a) şi 5ºC/min (b).*

The phase evolution of the precursor with calcinations temperature at 1000ºC for 6 h and samples sintered at 1450ºC and 1500ºC for 6 h is shown by means of XRD measurements (fig 3). It can be seen that the perovskite phase was identified in the pattern of the calcined samples, which is in agreement with the research results indicating that the perovskite phase transformation temperature is 1000ºC. Other intermediate phases including $LaSrGa_3O_7$, $La_4Ga_2O_9$, and some trace of carbonates were also detected.

$LaSrGa_3O_7$ crystallizes in a tetragonal structure of melilite-type ABC_3O_7. $LaSrGa_3O_7$ belongs to space group *P*-421*m* with the lattice parameters a_0 =8.056 Å and c_0=5.333 Å. [29]. According to phase-diagram studies [17, 19, 20]

$La_{1-x}Sr_{1-x}Ga_3O_7$ is the most stable high-temperature phase Ga_2O_3–La_2O_3–SrO system. The phase has extended coexistence regions with the following compounds: Ga_2O_3, (La,Sr)GaO_3, $SrGaO_{2.5}$, $Sr_3Ga_7O_{13.5}$, $LaSrGaO_4$, $LaSr_2Ga_{11}O_{20}$, $LaSr_3GaO_5$, and a liquid in the strontium rich part of the Ga_2O_3–SrO syst em[18]. The compound has a broad single-phase region at 1470°C in air (i.e., x = 0.20 to 0.60). When the lanthanum content is increased, the unit-cell volume decreases in size, particularly along the ***c***-axis.

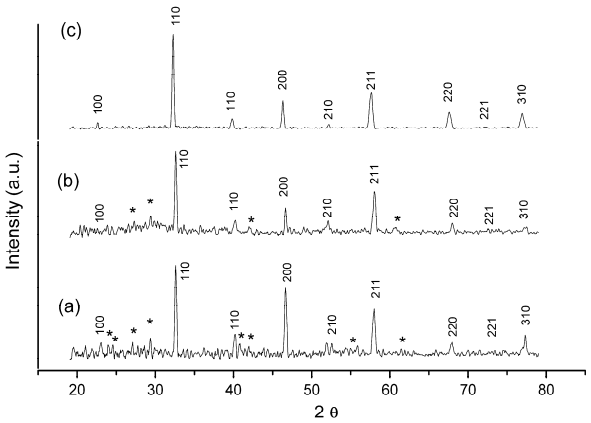

Fig. 3 - X-ray diffraction patterns of the calcined powders at 1000ºC/6h (a) and sintered ceramic (LSGM) after 1450 ºC/6h (b) and 1500ºC/6h annealing (c) / *Difractogramele amestecului stoichiometric calcinat la 1000ºC/6h (a) şi a ceramicii (LSMG) sinterizate la 1450 ºC/6h (b) şi 1500ºC/6h(c). (* $SrLaGa_3O_7$)*

No trace of impurity phases, i.e. $LaSrGa_3O_7$, were detected in the sample sintered in the temperature range of 1450ºC - 1500ºC for 6 h, which involve that the $LaSrGa_3O_7$ phase was removed (transformed) in the synthesis process of the Sr- and Mg-doped $LaGaO_3$. The indexed phase belong to a primitive cubic unit cell with a=3.9049 Å and V_o=59.545 $Å^3$, smaller than that reported by Huang *et al*. [21].

Further detailed researches have to be focused on this part of the subsolidus phase diagram of the doped La-Ga-O system.

It is well known that the powders synthesized through different synthesis routes have different properties, including morphology, particle size, specific surface area, etc., and so resulting in different sinterabilities. In fact, the loss of sinterability when increasing the calcinations temperature of the starting materials is well known among the ceramists. The powders used to prepare the green compacts were calcined at 1000ºC for 6 h and so higher temperature reduced the starting powders sinterability. It can be observed that the shrinkage ratio at 1500ºC was about 10%.

Figure 4.a presents the FTIR spectra of raw main materials. La_2O_3 spectrum presents absorption bands at 443, 643, 803, 1029, 1099,

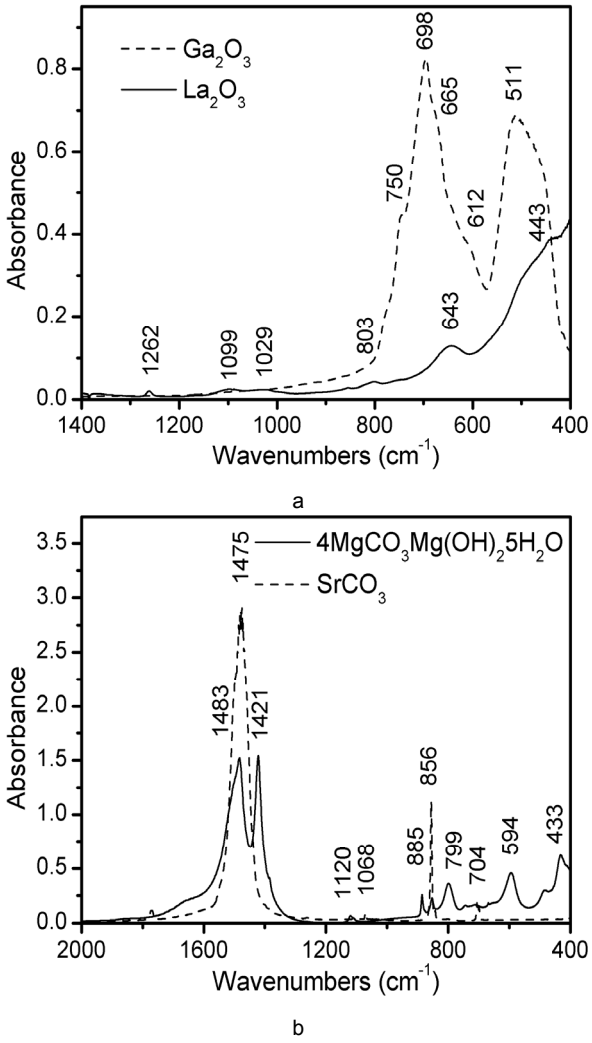

Fig.4 - FTIR spectra of raw materials: La_2O_3 and Ga_2O_3 – dotted line- (a) and $4MgCO_3Mg(OH)_2$ $5H_2O$ and $SrCO_3$ and–dotted line-(b) /*Spectul FTIR al materiilor prime: La_2O_3 şi Ga_2O_3-lina punctată (a) respectiv $SrCO_3$ şi $4MgCO_3Mg(OH)_2$ $5H_2O$-linia punctată(b).*

1262, 1457 and 3609 cm^{-1} respectively The absorption bands 643 cm^{-1} and 3609 cm^{-1} correspond to hexagonal $La(OH)_3$, which forms as a consequence of moisture absorption from air. The peak at 1457 cm^{-1}, 1099 cm^{-1}, 1029 cm^{-1} and 803 cm^{-1} corresponds to the stretching vibration of the carbonate group. The absorption band of cubic phase La_2O_3 appears at 520 cm^{-1} and 443 cm^{-1} Prominent IR absorption bands are observed at 458 cm^{-1}, 511 cm^{-1}, 665 cm^{-1}, 698cm^{-1}, 750 cm^{-1} in the case of Ga_2O_3. The bands located at 458 cm^{-1} and 511 cm^{-1} could be assigned Ga–O stretching vibration modes reported for β-Ga_2O_3. The peaks 665 cm^{-1} and 698 cm^{-1} are due to the presence of Ga–O bond vibrations. The shoulder at 750 cm^{-1} was noticed by Burkhalder [30] in FTIR spectra of Ga_2O_3 but not assigned to a specific vibration. Fig. 4b presents the IR spectra of doping precursors. The strong absorption band of CO_3^{2-}, centered at about 1475 cm^{-1} is characteristic for $SrCO_3$. Strong

narrow absorption bands at about 855 cm^{-1} and 704 cm^{-1} for $SrCO_3$, are assigned to be out of plane bending vibrations and in plane bending vibrations, respectively. Weak narrow absorption bands at about 1068 cm^{-1} due to the symmetric stretching vibrations were also detected.

The band located at 3448 cm^{-1} was assigned to OH^- group vibration in Mg precursor. The band at 1657 cm^{-1} was assigned to H_2O bending vibration of interlayer water in $4MgCO_3.Mg(OH)_2\ 5H_2O$. The ν_3 vibration of CO_3^{2-} in $MgCO_3$ was split in two signals, i.e., 1483 cm^{-1} and 1421cm^{-1}, and the ν_1 vibration band of CO_3^{2-} was observed at 1120 cm^{-1}. The absorption intensity below 550 cm^{-1} is probably attributable to octahedral magnesium.

Details about spectra of La_2O_3-Ga_2O_3 system are limited to those reported by Zhang et al. [31] and Saine *et al.*[32]. They have reported the infrared spectrum of the orthorhombic $LaGaO_3$ phase. The IR spectrum showed a total of 25 IR-active and 8 inactive modes for P*nma* (no.62) form and 8 IR-active and 5 inactive modes for R3*c* form, respectively.[33] The undoped $LaGaO_3$ undergoes a first-order phase transition from orthorhombic (P*bnm*) to hexagonal–rhombohedral (R3*c*) at

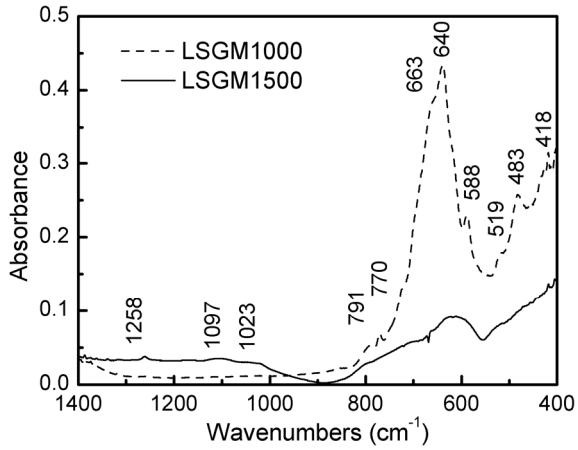

Fig. 5 - FTIR spectra of LSMG calcined powders at 1000ºC/6h – dotted line- and sintered samples at 1500ºC / *Spectrele FTIR ale pulberii de LSMG calcinate la 1000ºC/6h –linia punctată- şi al probelor sinterizate la 1500ºC/6h.*

approximate temperature of 150ºC. Slater et al. [11] have also shown that undoped $LaGaO_3$ undergoes a low temperature phase transition and the $La_{0.9}Sr_{0.1}Ga_{0.8}Mg_{0.2}O_{2.85}$ maintains monoclinic (I2/*a*) structure up to 1000ºC.

The bands observed in the spectrum (fig.5) can be assigned, by comparison of spectral profile and band positions, to the modes noticed for other perovskites. Assignments are made on the basis of the relative band positions. FT-IR spectra are in agreement with the XRD observations. The vibrations up to 1000 cm^{-1} are characteristic to perovskite structures. After pre-sintering the presence of CO_2 group's vibrations and traces of adsorbed water were also noticed. After sintering no vibrations were identified in the wave number range of 1300-4000 cm^{-1}

SEM images present the surface morphology of the sintered ceramic (fig.6a). Well-crystallized grains of polyedral shape are formed in the micrometric range in the normal ceramic microstructure with a good density. A grain to grain connectivity can be seen with average particle size 2-5 μm as shown in the higher magnification micrographs (fig. 6b). The presence of open porosity can be also observed (fig. 6b). This observation is in good agreement with the electrical behavior of the ceramic. These microstructures also explain the measured values for densities, porosities and the large shrinkage (~10% after sintering at 1500ºC/6h) of the sintered ceramics. Dilatometric tests on calcined samples confirmed that the active shrinkage processes, probably associated with cations interdiffusion, start at approximately 850-1000ºC. The results show a dependence between heating rate and shrinkage. That is, higher shrinkage (densification) is achieved at lower heating rates. This results yield fruitful information for the optimization of the process for such ceramics.

Fig 7 shows the dilatometric curves of LSGM ceramic undergoing a thermal cycle consisting of continuous heating and cooling The dilatometric curve shows linear thermal expansion characteristics in the investigated temperature

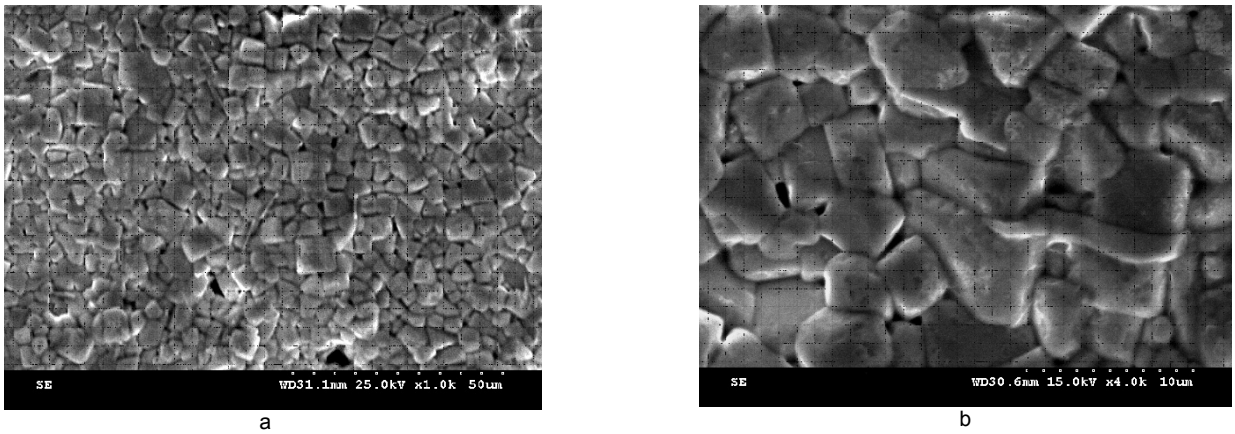

a b

Fig. 6 - Microstructural features of LSGM sintered ceramic at 1500ºC for 6h at two different magnifications / *Microstructura probelor LSMG de ceramică sinterizată la 1500ºC timp de 6 ore, la două scale diferite.*

range. The calculated thermal expansion coefficient (TEC) is 9.13 x 10^{-6} K^{-1} in the range 200-800ºC. The strain appearing (heating and cooling) indicates that the specimen length is change by the thermal cycle, which implies that the volume change has non-isotropic characteristics. It is well known that the elastic modulus and TEC have a major contribution to the stresses that can lead to cracking. If the difference in the TECs of surrounding components is large, its may crack during thermal cycling due to thermally induced stresses.

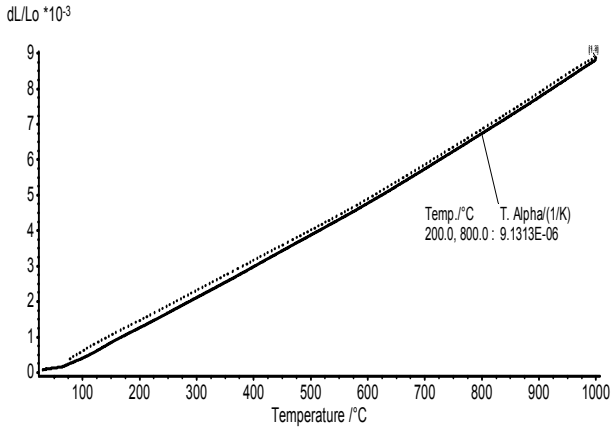

Fig 7 - Thermal expansion of the LSGM series; dotted line denotes the TEC values at cooling / *Coeficientul de expansiune termică al probelor de ceramică sinterizate; linia punctată reprezintă valorile CET înregistrate la răcire.*

The sintered ceramics were characterized by impedance spectroscopy (Wayne Kerr 6440A) at frequencies in the range 20 Hz – 3MHz with V_{ac} = 1 V. The measurements were carried out in air from room temperature up to 500°C. In Fig. 8 the imaginary part of the impedance is plotted versus the real part of the impedance for the sample heated at 300°C and 500°C, respectively.

At 300°C the spectra reveal two semicircles, which can be assigned to the diffusion of O^{-2} ion from vacancy to vacancy inside the grains (bulk process) and between two neighboring grains (grain boundary process). The semicircle from higher frequency corresponds to bulk process whereas the semicircle from lower frequency corresponds to grain boundary process.

To determine the dc-conductivity of the bulk and grain boundary, the semicircles of Nyquist plot in Fig. 8 were extrapolated to the intersections with the real axis, which gives the dc-resistances. In our case, the arcs are depressed with their centers displaced below the real axis; consequently the accuracy of simple extrapolation is not sufficient. The data have to be described with electrical equivalent circuits. It is not possible to fit the semicircle with the response of a simple RC - circuit (ideal semicircle with center on the real axis) because the bulk, as well as the grain boundary region exhibits a distribution of relaxation times

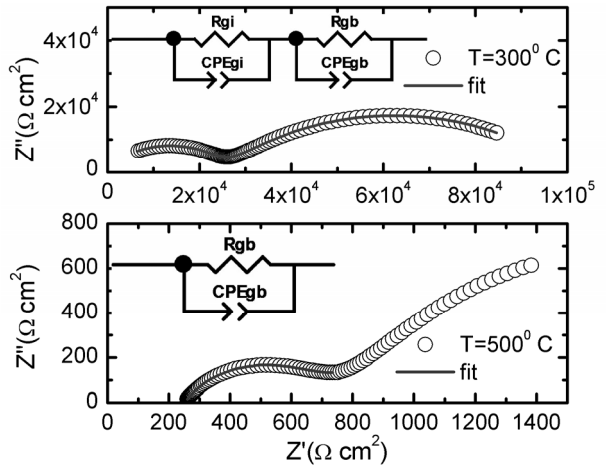

Fig 8 - Nyquist plots for sintered LSGM samples measured at 300°C and 500°C – open circles. The lines represent the fit of the experimental Nyquist plots with the response of the depicted electrical equivalent circuits / *Reprezentarea Nyquist a spectrelor de impedanță măsurate pe probele sinterizate de LSGM la temperatura de 300°C, respectiv 500°C – cercurile goale. Liniile reprezintă fitarea datelor experimentale cu circuitele electrice echivalente prezentate.*

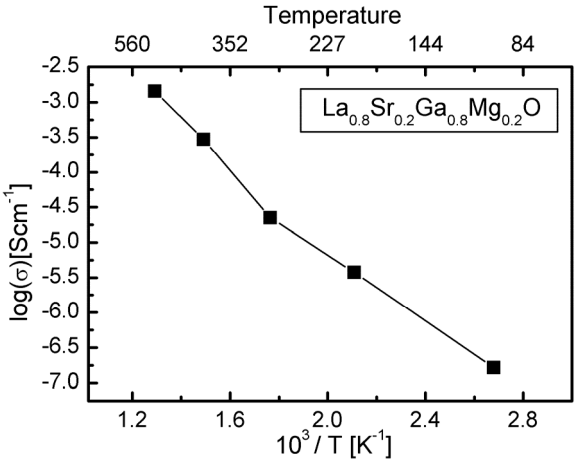

Fig. 9 - Temperature dependence of the conductivity of the LSGM ceramic sintered 6 h at 1500°C / *Variația conductivității cu temperatura a probelor ceramice de LSMG sinterizate 6 ore la 1500 °C.*

(both centers below the real axis). This behavior can be described by a RC-circuit, in which the capacitor is exchanged by a "constant phase element" (CPE). The impedance of the CPE is given by the following equation:

$$Z_{CPE} = A(i\omega)^{-b},$$

where ω is the angular frequency and A and $b \in [0,1]$ are frequency independent constants. An example of the result of a fit is shown in the Fig. 8 for sample measured at 300°C and 500°C. *The fit (continuous line) describes not only the shape and absolute values of the measured data (open circles) but also the frequency dependence of the data.*

From fitting data with the equivalent circuit depicted in figure 8 is observed that, at 300°C, the

grain boundary resistance (R_{gb} ~ 6.4 x 10^4 Ω) is considerable higher than the grain bulk component (R_b ~ 3 x 10^4 Ω).

At 500 °C the semicircle corresponding to the bulk contribution is out with respect to the frequency scale of instrumentation. The remained large semicircle corresponds to the grain boundary impedance ~ 6 x 10^2 Ω and the low frequency spike inclined at ~45° is associated with diffusion of oxygen molecules at the contact.

Figure 9 shows the Arrhenius representation of total electrical conductivity of the sample sintered at 1500°C for 6 h. The lower values, compared with the published one [2,3] can be due to the microstructure of the sintered ceramic (grain boundary conduction effect).

4. Conclusion

A specific solid state preparation method was used to obtain Sr and Mg doped $LaGaO_3$ ceramics, starting from oxides and carbonates. Different heating rate for carbonates decomposition were used. The dopans were gradually released in the system.

Detailed structural investigation demonstrates the obtaining of a well-crystallized ceramics of cubic symmetry in the range of 1450ºC-1500ºC.

The structure and the morphology of the obtained ceramic may explain also the electrical behavior of the grain boundary resistance (R_{gb}) which is considerable higher than the grain bulk component (R_b).

Further investigation on the mechanism of reaction and the phase equilibrium of the doped La-Ga-O system and also on sintering process are necessary.

Acknowledgement

This work was supported by CNMP PNII project 71030/2007 and CNCSIS-UNIFISCU project number PNII-RU 196/2010.

REFERENCES

1. T. Ishihara, H. Matsuda, and Y. Takita, Doped $LaGaO_3$ perovskite type oxide as a new oxide ionic conductor, J. Am. Chem. Soc. 1994, **116**, 3801.
2. M. Feng and J.B. Goodenough, A superior oxide-ion conductor, Eur. J. Solid State Inorg. Chem. 1994, **31**, 663.
3. V.V. Khartona, F.M.B. Marquesa, and A. Atkinson, Transport properties of solid oxide electrolyte ceramics: a brief review, Solid State Ionics 2004, **174**, 135.
4. I. Yasuda, Y. Matsuzaki, T. Yamakawa, and T. Koyama, Electrical conductivity and mechanical properties of alumina-dispersed doped lanthanum gallates, Solid State Ionics 2000,**135**, 381.
5. J.-H. Kim, and H.-I. Yoo, Partial electronic conductivity and electrolytic domain of $La_{0.9}Sr_{0.1}Ga_{0.8}Mg_{0.2}O_{3-\delta}$, Solid State Ionics 2001, **140**, 105.
6. J.W. Stevenson, T.R. Armstrong, L.R. Pederson, J. Li, C.A. Levinsohn, and S. Baskaran, Effect of A-site cation nonstoichiometry on the properties of doped lanthanum gallate, Solid State Ionics 1998, **113–115**, 571.
7. P. Huang, and A. Petric, Superior Oxygen Ion Conductivity of Lanthanum Gallate Doped with Strontium and Magnesium, J. Electrochem. Soc. 1996, **143**, 1644.
8. V.V. Kharton, A.P. Viskup, E.N. Naumovich, and N.M. Lapchuk, Mixed electronic and ionic conductivity of $LaCo(M)O_3$ (M = Ga, Cr, Fe or Ni): I. Oxygen transport in perovskites $LaCoO_3$–$LaGaO_3$, Solid State Ionics 1997, **104**, 67.
9. T. Ishihara, M. Higuchi, H. Furutani, T. Fukushima, H. Nishiguchi, Y. Takita, Potentiometric oxygen Sensor Operable in Low-Temperature by Applying $LaGaO_3$-Based Oxide for Electrolyte, J. Electrochem. Soc. 1997, **144**, L122.
10. T. Ishihara, J.A. Kilner, M. Honda, N. Sakai, H. Yokokawa, and Y. Takita, Oxygen surface exchange and diffusion in $LaGaO_3$ based perovskite type oxide, Solid State Ionics 1998, **113–115**, 593.
11. P.R. Slater, J.T.S. Irvine, T. Ishihara, and Y. Takita, The Structure of the Oxide Ion Conductor $La_{0.9}Ga_{0.1}Mg_{0.2}O_{2.85}$ by powder neutron diffraction, Solid State Ionics 1998, **107**, 319.
12. K. Yamaji,T. Horita, M. Ishikawa, Natsuko S. and H. Yokokawa, Chemical stability of the La0.9Sr0.1Ga0.8Mg0.2O2.85 electrolyte in a reducing atmosphere. Solid State Ionics, 1999. **121**(1-4), 217.
13. M. Preda, A. Melinescu, Cerium oxide sintering using strontium oxide as additive, Roumanian Journal of Materials, 2009, **39** (1), 50.
14. E. Djurado and M. Labeau, Second phases in doped lanthanum gallate perovskites. Journal of the European Ceramic Society, 1998. **18**(10), 1397.
15. K.Q.Huang, R.S.Tichy, J. B.Goodenough, Superior Perovskite Oxide-Ion Conductor; Strontium- and Magnesium-Doped $LaGaO_3$: III, Performance Tests of Single Ceramic Fuel Cells , J.Am.Ceram.Soc. 1998, **81**(10), 2581.
16. K.Q.Huang, R.S.Tichy, J.B.Goodenough, Superior Perovskite Oxide-Ion Conductor; Strontium- and Magnesium-Doped $LaGaO_3$: I, Phase Relationships and Electrical Properties, J.Am.Ceram.Soc, 1998, **81**(10), 2565.
17. P. Majewski, M. Rozumek, and F. Aldinger, Phase diagram studies in the systems La_2O_3-SrO-MgO-Ga_2O_3 at 1350-1400° C in air with emphasis on Sr and Mg substituted $LaGaO_3$, J. Alloys Compd., 2001, **329**, 253.
18. V.P. Gorelov, D.I. Bronin, Ju.V. Sokolova, H. Nafe, and F. Aldinger, The effect of doping and processing conditions on properties of $La_{1-x}Sr_xGa_{1-y}Mg_yO_{3-\alpha}$, J. Eur. Ceram. Soc. 2001, **21**, 2311.
19. M. Rozumek, P. Majewski, L. Sauter, and F. Aldinger, Homogeneity region of strontium- and magnesium-containing $LaGaO_3$ at temperatures between 1100 and 1500C in air, J. Am. Ceram. Soc., 2003, **86** (11), 1940.
20 M. Rozumek, P. Majewski, and F. Aldinger, Metastable crystal structure of strontium- and magnesium-substituted $LaGaO_3$, J. Am. Ceram. Soc., 2004, **87** (4), 662.
21. K. Huang, R.S. Tichy, and J.B. Goodenough, Superior Perovskite Oxide-Ion Conductor; Strontium- and Magnesium-Doped $LaGaO_3$: I, Phase Relationships and Electrical Properties, J. Am. Ceram. Soc. 1998, **81**, 2565.
22. K.T. Lee, S.Kim, G.D.Kim, and H.L.Lee, J.Appl. Electrochem. 2001, **31,** 1243.
23. O.Schultz, M.Martin, C.Argiruris, and G.Borchard, Cation tracer diffusion of ^{138}La, ^{84}Sr and ^{20}Mg in polycrystalline $La_{0.9}Sr_{0.1}Ga_{0.9}Mg_{0.1}O_{2.9}$, Phys.Chem.Chem.Phys, 2003, **5,** 2308.
24. D. Radu and C. Mazilu, Temperature influence at the oxides basicity**,** Romanian Journal of Materials 2009, **39** (2), 156.

25. J. J. Lander, ''Polymorphism and Anion Rotational Disorder in the Alkaline Earth Carbonates,'' J. Chem. Phys., 1949 **17**, 892.
26. M. Sweeney, ''Thermal Stabilities of Isoelectronic, Isostructural Nitrates, Carbonates and Borates,'' Thermochim. Acta, 1975, **11**, 409.
27. Y. L. Chang and H. I. Hsiang, M.T. Liang, Phase Evolution During Formation of $SrAl_2O_4$ from $SrCO_3$ and alpha-Al_2O_3/AlOOH, J. Am. Ceram. Soc., 2007, **90,** 2759.
28. Y. Sawada, J. Yamaguchi, O. Sakurai, K. Uematsu, N. Mizutani and M. Kato**,** Thermogravimetric study on the decomposition of hydromagnesite 4 $MgCO_3.Mg(OH)_2$ x4 H_2O, Thermochimica Acta, 1979, **33,** 127.
29. M. Stein, W. Schmitz, R. Uecker, and J. Doerschel, Crystal structure of strontium lanthanum trigallium heptoxide, $(Sr_{0.5}La_{0.5})_2Ga_3O_7$, Z. Kristallogr.-New Cryst. Struct., 1997, **12**, 212.
30. T.R. Burkholder, T.J. Yustein and L.J. Andrews. "Reactions of Pulsed Laser Evaporated Ga and In Atoms with Molecular Oxygen. Matrix Infrared Spectra of New GaO_2 and InO_2 Species" J. Phys. Chem., 1992, **96**, 10189.
31. Z.M.Zhang, B.J.Choi, M.I. Flik and A.C.Amderson, Infrared refractive indices of $LaAlO_3$, $LaGaO_3$, and $NdGaO_3$, J.Opt.Sos. Am. B11, 1994, 2252.
32. M.C.Saine, E.Husson and H.Brusset, Etude vibra-tionnelle d'aluminates et de gallates de terres rares—II. Gallates de structure perovskite, Spectrocehem.Acta Part A37, 1981 985.
33. G.A.Tompset, N.M.Sammes and R.J.Phillips, Raman Spectroscopy of the $LaGaO_3$ Phase Transition, J Raman Spectr. 1999, **30**, 497.

****

MANIFESTĂRI ŞTIINȚIFICE / SCIENTIFIC EVENTS

12th Conference of the European Ceramic Society (ECerS XII)

19-23.06.2011, Stockholm, Sweden

General Themes

The conference will cover the entire field of ceramic science and Technology. The presentations will be grouped within broadly defined general sessions.

- Bioceramics
- Composites, Coatings and Engineering Ceramics
- Electroceramics and Solid Oxide Fuel Cells
- Innovative Processing and Synthesis
- Nanomaterials
- Silicates, Refractories, Cements and Traditional Ceramics
- Art and Design

Topical Symposia

In addition to the general themes, seven sessions with a more specific focus will be organised.

- Transparent Ceramics
- Advancements and Innovation in Polymer-derived Ceramics
- Advanced Ceramics and Ceramic Processes for Dentistry
- Multilayer Ceramics
- Ceramic Membranes and Adsorbents
- Science and Technology of Anisotropic Ceramics
- Ceramic Processing Science using Lasers

Contact: http://www.ecers2011.se
Questions regarding the scientfic programme: Email: info@ecers2011.se
Questions regarding registration, accommodation and social programme
MCI Stockholm Office
P O Box 6911
SE-102 39 Stockholm
Tel: +46 8 5465 1500
Send email: www.mci-group.com

****